LBL-12770
c.2

Lawrence Berkeley Laboratory
UNIVERSITY OF CALIFORNIA

ENERGY & ENVIRONMENT DIVISION

Presented at the Eighteenth International Symposium on Combustion, University of Waterloo, Waterloo, Ontario, Canada, August 17-22, 1980; and to be published in the Proceedings

OPPOSED FLOW DIFFUSION FLAME EXTENSIONS

C.M. Kinoshita, P.J. Pagni, and R.A. Beier

May 1981

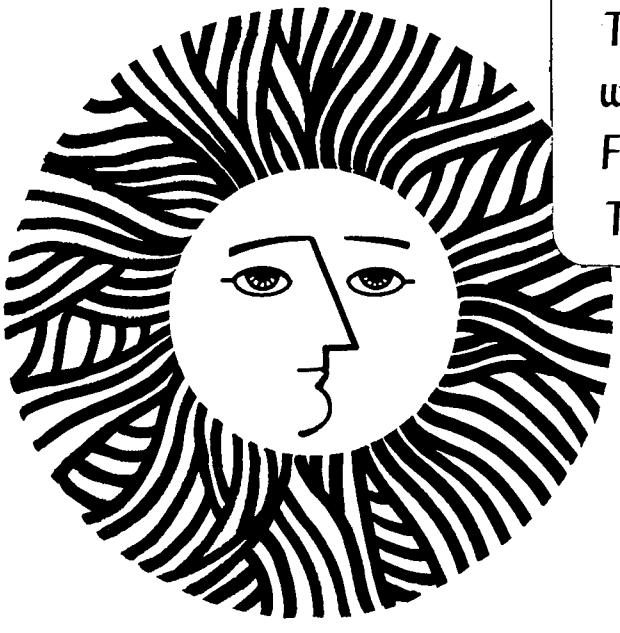

Prepared for the U.S. Department of Energy under Contract W-7405-ENG-48

LBL-12770
c.2

DISCLAIMER

OPPOSED FLOW DIFFUSION FLAME EXTENSIONS

C. M. Kinoshita, P. J. Pagni and R. A. Beier

Mechanical Engineering Department
and
Lawrence Berkeley Laboratory
University of California
Berkeley, California 94720 U.S.A.

Abstract

The Opposed Flow Diffusion Flame (OFDF) apparatus has been used for estimating the thermochemical properties of materials related to fire safety and for diffusion flame structure studies. Here the extension of the flame beyond the pyrolyzing fuel surface and the excess pyrolyzate are predicted. Since flame and stagnant plane locations may be sensitive to the usual Le = 1 assumption, these additional predictions which are not so sensitive can provide useful estimates of fuel properties. Shvab-Zeldovich variables are used in analysis of steady, laminar, non-radiative, axi-symmetric and Cartesian two-dimensional boundary layers. The thin diffusion flame lies within the boundary layer on the oxidant side of the stagnation plane. Much of the behavior of the velocity, enthalpy and species profiles is similar to the analogous free convection flame profiles. The results depend on five parameters: r, the mass consumption number; B, the mass transfer number; D_c, a dimensionless heat of combustion; θ_w, the fuel surface temperature; and Pr, the Prandtl number. The fuel pyrolysis rate is controlled primarily by B, while the flame extension is dominated by r and the flame temperature is influenced by D_c. In comparison with polymer experiments, care is required to insure that the apparatus satisfies the model assumptions and that radiative emission from the fuel surface is taken into account. Good agreement is obtained between predicted and experimental flame extensions for polymethylmethacrylate.

This manuscript was printed from originals provided by the author.

Introduction

Opposed flow diffusion flame (OFDF) apparati provide well controlled systems used in flame structure studies [1-4] and employed in estimating thermochemical properties of materials related to fire safety [5,6]. Fuel pyrolysis, excess pyrolyzate, and the downstream extent of the flame are emphasized here. Since the flame extent is easily measured, it may provide a useful additional means to ascertain material properties. A stream of gas phase oxidizer in stagnation-point flow approaches a condensed fuel surface and forms a constant thickness boundary layer containing a thin diffusion flame. The oxidizer reacts there with pyrolyzed fuel and then flows downstream along an inert, adiabatic surface carrying products and unburned fuel. The system separates naturally at the end of the fuel surface into two regions shown schematically in Fig. 1: (1) a pyrolysis region where the fuel gasifies in response to heat transfer from the flow and is partially consumed; and (2) an extended flame region downstream of the fuel source where the combustion process continues to completion after pyrolysis has ceased.

Steady, laminar, non-radiative, stagnation-pooint flow in both axi-symmetric and Cartesian configurations is considered. It is assumed that the boundary-layer approximations are valid with the free stream specified by potential [7] or rotational [8] flow. Shvab-Zeldovich variables are employed to predict detailed velocity, species and temperature profiles for the pyrolysis region, and the fraction of locally unburned pyrolyzed fuel which is convected downstream, i.e., the "excess pyrolyzate" [10-12]. The similarity formulation for the pyrolysis region is abbreviated since it resembles an excellent previous analysis [13].

Downstream of the pyrolysis region, the flame is sustained by pyrolyzate not consumed upstream. Similarity is no longer valid in this region due to the abrupt change in boundary conditions at the fuel-inert border, hence finite difference analyses are employed to calculate the remaining pyrolyzate and the extent of the flame.

Pyrolysis Region

Analyses

Let x and y denote orthogonal spatial coordinates tangential and normal to the fuel surface, respectively, as illustrated in Fig. 1. The free-stream velocities are u_∞ and v_∞ in the x- and y-directions, respectively. Several alternatives exist to approximate the free-stream in an OFDF apparatus [7-9]. Since the fuel velocity at the pyrolyzing surface is much less than the oxidant nozzle velocity, only $\partial u_\infty/\partial x$ is of importance [9] and the development which follows applies to all alternatives with u_∞ linearly dependent on x. Near the surface, viscous, blowing and combustion effects are accounted for with the usual boundary-layer and Shvab-Zeldovich assumptions. The continuity, momentum, and coupled energy-species equations, neglecting dissipation and radiation are

$$\frac{\partial}{\partial x}\ (\rho u x^K)\ +\ \frac{\partial}{\partial y}\ (\rho v x^K)\ =\ 0 \qquad (1)$$

$$\rho u \frac{\partial u}{\partial x} + \rho v \frac{\partial u}{\partial y} = \frac{\partial}{\partial y} \left(\mu \frac{\partial u}{\partial y}\right) + \rho_\infty u_\infty \frac{\partial u_\infty}{\partial x} \tag{2}$$

$$\rho u \frac{\partial J}{\partial x} + \rho v \frac{\partial J}{\partial y} = \frac{\partial}{\partial y} \left(\rho D \frac{\partial J}{\partial y}\right) \tag{3}$$

in which $\kappa = 0$ for Cartesian flow and $\kappa = 1$ for axisymmetric flow, and J is the normalized energy-species variable. The conventional transformation is

$$\eta \equiv \left(\frac{u_\infty}{\nu_\infty x}\right)^{\frac{1}{2}} \int_0^y \frac{\rho}{\rho_\infty} \, dy \, . \tag{4}$$

Note that here, η is independent of x. The usual stream function used to satisfy continuity

$$\frac{\partial \psi}{\partial y} = \frac{\rho u x^\kappa}{\rho_\infty} \, , \quad \frac{\partial \psi}{\partial x} = - \frac{\rho v x^\kappa}{\rho_\infty} \tag{5a}$$

is non-dimensionalized as

$$f(\eta) \equiv \frac{\psi}{(\nu_\infty u_\infty x)^{\frac{1}{2}} \, x^\kappa} \, , \tag{5b}$$

so that $f'(\eta) = u/u_\infty$.

Assuming constant Prandtl number, constant $\rho\mu$, and uniform molecular weight across a boundary layer composed of an ideal gas mixture, gives the following transformed momentum and energy-species equations

$$f''' + (\kappa + 1) \, ff'' - (f')^2 + \theta = 0 \tag{6}$$

and

$$J'' + (\kappa + 1)\, PrfJ' = 0 \quad , \tag{7}$$

where $\theta \equiv T/T_\infty = \rho_\infty/\rho$, and prime denotes differentiation with respect to η. The flow boundary conditions,

$$f'(0) = 0, \quad f'(\infty) = 1, \quad f(0) = \frac{B}{(\kappa + 1)\, Pr}\, J'(0) \tag{8}$$

are no-slip, free-stream, and surface mass flux proportional to heat flux, respectively. The energy-species conditions are, by definition:

$$J(0) = 1, \quad J(\infty) = 0 \quad . \tag{9}$$

Species and temperature fields are

$$Y_o/Y_{o\infty} = 0, \quad Y_f/Y_{fw} = (1 + r)\, J - r,$$

$$\theta = (\theta_w - 1)\, [D_c - (D_c - 1)\, J] + 1, \quad \eta < \eta_{f\ell} \tag{10a}$$

and

$$Y_f/Y_{fw} = 0, \quad Y_o/Y_{o\infty} = 1 - \left(\frac{1 + r}{r}\right) J \ ,$$

$$\theta = (\theta_w - 1)\, [1 + D_c/r]\, J + 1, \quad \eta > \eta_{f\ell} \tag{10b}$$

where constant specific heat is assumed. At the flame, $J_{f\ell} = r/(1 + r)$ and $\theta_{f\ell} = (\theta_w - 1)\, (D_c + r)/(1 + r) + 1$.

The total pyrolysis rate is the cumulative flux of pyrolyzate leaving the surface:

$$\dot{M}_p \equiv \int_0^x x^K \rho_w v_w \, dx \tag{11a}$$

while the excess pyrolyzate is the total fuel convected downstream between the pyrolyzing surface and the flame:

$$\dot{M}_e \equiv \int_0^{y_{f\ell}} x^K \rho u Y_f \, dy \quad . \tag{11b}$$

The local pyrolysis rate can be written as

$$\dot{m}_p'' \equiv \rho_w v_w = - (K + 1) \rho_\infty \left(\frac{\nu_\infty u_\infty}{x}\right)^{\frac{1}{2}} f(0) \quad , \tag{12}$$

so that from equations (11a and 12)

$$\dot{M}_p = - \rho_\infty \left(\frac{\nu_\infty u_\infty}{x}\right)^{\frac{1}{2}} x^{K+1} f(0) \quad . \tag{13}$$

The unburned fraction of the total fuel pyrolyzate is thus

$$\frac{\dot{M}_e}{Y_{ft} \dot{M}_p} = \frac{Br}{B + r + 1} \frac{\int^{\eta_{f\ell}} f'(J/J_{f\ell} - 1) \, d\eta}{- f(0)} \quad . \tag{14}$$

Results

The system of ordinary differential equations (6 and 7), and boundary conditions, (8 and 9), was solved with the non-iterative parametric expansion method [14] for f and J over the following ranges of the five parameters which specify the results in this study: the Prandtl number, Pr = 0.73, the mass transfer number, $0.1 \leqslant B \leqslant 10$, the mass consumption number, $0.1 \leqslant r \leqslant 1.0$, a dimensionless heat of combustion, $D_c = 4.0$, and the dimensionless surface temperature, $\theta_w = 2.0$. The fixed values of the less significant parameters are typical of solid polymer fuels.

As in other systems, [10-12], the pyrolysis rate depends primarily on B. Simultaneous increases in both the flame stand-off distance and flame temperature as r decreases (see Fig. 2b) cause the temperature profile near the surface, hence conduction and pyrolysis, to vary only slightly with r. The pyrolysis rates are well fit over the ranges listed above by

$$- f(0) = 0.543\, r^{-0.02}\, B^{0.626}\, B^{-0.0678\, \ell n\, B} \qquad (15a)$$

and

$$- f(0) = 0.353\, r^{-0.02}\, B^{0.611}\, B^{-0.0651\, \ell n\, B} \qquad (15b)$$

for Cartesian and axisymmetric cases, respectively. The D_c, θ_w and Pr dependence is too weak to include; these expressions should be valid for all fuels.

Figures 2a and 2b plot velocity and temperature profiles in the pyrolysis region of axisymmetric OFDF's for various mass transfer numbers, B, and mass consumption numbers, r. As expected, Fig. 2a shows decreasing velocity gradients near the wall with increasing B number due to increased pyrolysis. With combustion, the velocity in the boundary layer exceeds its free-stream value with a maximum near the flame similar to the velocity profile of combusting, forced and free, mixed-mode convective flows [11,12]. This velocity "overshoot" in the boundary layer is caused by the favorable pressure gradient coupling with the high gas temperature in the boundary layer [13]. Figure 2b illustrates that the flame temperature is independent of B for specified D_c, r and θ_w, and that the flame location is strongly dependent on r. A comparison of both figures shows that the degree of velocity overshoot grows as the flame temperature increases. The maximum velocity is generally located outside the flame sheet for high r numbers and inside for more common low r numbers; Fig. 2b gives the flame location at θ_{max}.

Figure 3 gives the location of the stagnation (v = 0) plane, η_{sp}, and flame stand-off distance, $\eta_{f\ell}$, as functions of B, parameterized in r, for axisymmetric flow. The increase in pyrolysis rate as B increases causes the outward displacement of the stagnation plane and the flame. The dependence of η_{sp} on r, like the pyrolysis rate, is negligible. Since the flame sheet moves away from the fuel surface as the relative available oxygen decreases, $\eta_{f\ell}$ increases with decreasing r.

The stagnation plane generally lies inside the flame sheet, hence, convection aids diffusion of fuel out to the stagnation plane, but opposes fuel diffusion thereafter. Diffusion of oxidizer into the reaction zone is always aided by convection due to the inward directed

flow component, which also increases as ρ decreases in the flame [2,3]. On the fuel side, $v(\eta)$ decreases monotonically from the value given by Eq.(15)at the fuel surface to 0 at the stagnation plane. Cartesian combustion is analogous to axisymmetric combustion in every respect.

Figure 4, which underscores the role of the mass consumption number, r, in excess pyrolyzate, plots the fraction of unburned pyrolyzate versus B parameterized in r. As the oxygen in the free-stream drops (i.e., as r decreases) more excess pyrolyzate results. A less pronounced increase in unburned fraction with B number is also observed. In analogy with mixed flows, the velocity overshoot produces a relatively high streamwise flow near the surface, enhancing downstream fuel convection and producing an unburned fraction slightly higher than forced, but slightly lower than free flow [10-12].

Downstream Combustion Analyses

Due to the abrupt change in boundary conditions at the downstream end of the pyrolyzing surface , the similarity solution developed for the pyrolysis region no longer applies, hence GENMIX [15-17] was used. An integral analysis was found to be inadequate when compared with finite difference results as in other flow systems [10-12]. The appropriate dimensionless variables for downstream combustion are:

$$X \equiv \frac{x}{\ell} \quad , \quad Z \equiv \frac{Re_\ell^{\frac{1}{2}}}{\ell} \int_0^y \frac{\rho}{\rho_\infty} \, dy \quad , \tag{16a}$$

$$U \equiv \frac{u}{u_{\infty \ell}} \quad , \quad V \equiv \frac{Re_{\ell}^{\frac{1}{2}}}{\rho_{\infty} u_{\infty \ell}} \left(\rho v + u \int_{o}^{y} \frac{\partial \rho}{\partial x} \, dy \right) \tag{16b}$$

in which $Re_{\ell} \equiv (u_{\infty \ell} \, \ell)/\nu_{\infty}$. The governing equations become

$$\frac{\partial}{\partial X} (UX^{K}) + \frac{\partial}{\partial Z} (VX^{K}) = 0 \tag{17a}$$

$$U \frac{\partial U}{\partial X} = V \frac{\partial U}{\partial Z} = \frac{\partial^2 U}{\partial Z^2} + X\theta \tag{17b}$$

$$U \frac{\partial J}{\partial X} + V \frac{\partial J}{\partial Z} = \frac{1}{Pr} \frac{\partial^2 J}{\partial Z^2} \tag{17c}$$

with the following boundary conditions:

$$U = 0, \; V = - \frac{B}{Pr} \frac{\partial J}{\partial Z} \quad , \quad J = 1 \text{ at } Z = 0, \quad X < 1 \tag{18a}$$

$$U = V = \frac{\partial J}{\partial Z} = 0 \quad \text{at } Z = 0, \quad X > 1 \tag{18b}$$

and

$$U = X, \quad J = 0 \quad \text{as } Z \to \infty \, . \tag{18c}$$

The unburned fraction of total fuel pyrolyzate is found from Eqs. (11 and 16) as

$$\frac{\dot{M}_e}{Y_{ft}\,\dot{M}_P} = \frac{Br}{B + r + 1}\;\frac{\int_0^{Z_{f\ell}} U(J/J_{f\ell} - 1)\,dZ}{\int_0^{X} V_w\,dX} \quad . \tag{19}$$

The flame extension is obtained implicitly from $J(X_{f\ell},0) = J_{f\ell}$, i.e., where the flame sheet intersects the surface. Since Re_ℓ does not appear either in the defintion of X or the dimensionless governing Eqs. (17-19), both the downstream unburned fraction of pyrolyzate and flame extension are independent of Re_ℓ. The dimensionless equations verify that, analogous to forced and free flow combustion of a fuel slab [10,12,17], no new parameters emerge from the analysis of the extended flame zone.

Results

GENMIX calculations traversed both the pyrolysis region and the extended flame zone as previously described [12,17]. Wall gradients at the downstream edge of the fuel surface calculated with GENMIX compared well with upstream similarity values as a check on the numerics.

Figure 5 plots the dimensionless flame extension, $X^*_{f\ell} \equiv X_{f\ell} - 1$, as a function of mass transfer number, B, parameterized in mass consumption number, r. The dominant role that the mass consumption number, r, plays in the amount of excess pyrolyzate produced upstream (Fig. 4) is reflected in its strong influence on flame length downstream. It is apparent that low r number fuels produce long flames.

As expected shorter flames are obtained in axisymmetric systems than in Cartesian systems due to the increase in downstream flow area. Stagnation-point flames are shorter than wake flames [12] because u_∞ increases in the former and remains constant in the latter. Since in both cases the total convection flux of J in the extended flame zone is fixed, J must decay faster in the stagnation-point flow.

Other GENMIX calculations indicate that over their range of typical values, the influence of D_c and θ_w on both unburned fraction of pyrolyzate and flame extension is slight which is somewhat expected as both D_c and θ_w enter the analysis primarily through θ in the momentum equation.

Table I shows, in order of increasing r number, pyrolysis rate, excess pyrolyzate and flame length predictions for selected materials burning in air with estimates of r, B, D_c and θ_w based on available data [18,19]. Stoichiometric coefficients are approximated by complete combustion of the monomer. Column 7 tabulates the local pyrolysis rate, $-f(0)$, which, via Eq. (13), permits immediate evaluation of the total pyrolysis rate, $\dot{M}_p$. Column 8 presents the unburned fraction of pyrolyzate for the pyrolysis region. Flame extensions obtained with GENMIX are listed in the last column.

Comparisons with Experiment

Flame extensions in axisymmetric polymethylmethacrylate (PMMA) OFDF's burning in O_2/N_2 mixtures were measured experimentally. Details of the OFDF apparatus have been given [4]. Fuel rod and oxidizer nozzle diameters were 1.27 and 2.54 cm, respectively. $Y_{O\infty}$ was varied from 30 to 100 percent producing B numbers from 2 to 8 and r numbers from 0.25 to 0.65. Figure 6 plots the dimensionless flame extension, $X^*_{f\ell} = X_{f\ell}/\ell$, where ℓ is the sample radius, versus free-stream oxygen mass fraction, $Y_{O\infty}$, for a constant nozzle exit velocity, $V_O \simeq 1.3$ m/s. Measurements at other velocities show that, consistent with theory, the flame extension is quite independent of free-stream Reynolds number, Re_ℓ. The agreement between theory and experiment is good. Experimental flame extensions may be slightly effected by radiation from the pyrolyzing fuel surface, which lowers B and through Y_{fw} increases r. The data scatter is due primarily to the difficulty of identifying the radius of the melted, pyrolyzing PMMA. As in wall-wake combustion [12], the flame extension decreases as $Y_{O\infty}$ increases primarily because of an increase in r, in spite of a simultaneous increase in B. Since the flame length is easily measured and is independent of the free-stream, it may prove a useful additional means to ascertain material properties.

It is important that an OFDF apparatus be constructed and operated so that theoretical assumptions are properly represented. The distance from the nozzle exit to the pyrolyzing surface, ℓ_O, should be large compared to the boundary layer thickness, δ, i.e., $Re \equiv V_O \ell_O/\nu_\infty >> 1$ since $\delta/\ell_O \sim Re^{-\frac{1}{2}}$ [20]. Here Re = 130 and is barely adequate. In evaluating the B number from measured pyrolysis rates, $\dot{m}''_p$ using Eqs.

(12 and 15), it is required to use the actual area of the pyrolyzing surface, not the fuel rod cross-section. For melting materials, e.g., PMMA, polyethylene [4], etc., using the rod area may overestimate B. For very strongly sooting materials like polystyrene, soot accumulation could restrict the pyrolysis surface area to less than the rod cross-section, causing B to be underestimated [5]. Radiation effects are discussed elsewhere [21]. Attention should also be paid to the details of the nozzle shape and size since that defines the free-stream condition.

The simplest free-stream is given by stagnation point potential flow [7]

$$\frac{u_\infty}{V_o} = \left(\frac{1}{\kappa + 1}\right) \frac{x}{\ell_o} \quad , \quad \frac{v_\infty}{V_o} = - y/\ell_o \tag{20}$$

For the axisymmetric case with normal, uniform injection, Seshadri and Williams [9] show that rotational, inviscid flow between infinite plates gives

$$\frac{u_\infty}{V_o} = \frac{x}{\ell_o} \left(1 - \frac{y}{\ell_o}\right) \quad , \quad \frac{v_\infty}{V_o} = \left(\frac{y}{\ell_o}\right)^2 - 2 \left(\frac{y}{\ell_o}\right) \quad . \tag{21}$$

Proudman [8] discusses the Cartesian form of Eq. (21). Since most OFDF apparati constrain u_∞ to be zero and v_∞ to be uniform, i.e., V_o, across the nozzle exit plane, Eq. (21) is the more appropriate free-stream flow.

Conclusions

Excess pyrolyzate and flame extensions in laminar OFDF's are predicted. Five parameters, the Prandtl number, Pr, the mass transfer number,

B, the mass consumption number, r, a dimensionless heat of combustion, D_c, and the dimensionless surface temperature, θ_w, emerge from this study. The OFDF apparatus may be used to quantify some of these parameters. B is usually obtained from pyrolysis data. The extent of the flame may be used to determine r, which has been shown to be an important parameter in assessing material fire hazard. Measurement of $T_{f\ell}$ and T_w yields D_c. The flame and stagnation-plane locations may be employed as checks on r and B, respectively. Much of the behavior of the velocity, temperature and species profiles is similar to free convection flame profiles. Good agreement is obtained between experimental and predicted flame extensions.

NOMENCLATURE

A = u_∞/x

B = mass transfer number, $(QY_{o\infty}/\nu_o W_o - h_w)/L$

c_p = specific heat

D = species diffusivity

D_c = dimensionless heat of combustion, $QY_{o\infty}/\nu_o W_o h_w$

f = dimensionless stream function

h = specific enthalpy, $\int_{T_\infty}^{T} c_p dT$

J = normalized Shavab-Zeldovich coupling variable, $(\beta-\beta_\infty)/(\beta_w-\beta_\infty)$

L = effective latent heat of pyrolysis

ℓ = fuel length

$\dot{m}''$ = mass flux

Pr = Prandtl number

Q = energy released by combustion of ν_f moles of gas phase fuel

$\dot{q}''$ = heat flux

Re_x = Reynolds number, $u_\infty x/\nu_\infty$

r = mass consumption number, $Y_{o\infty}s/Y_{fw}$

s = stoichiometric ratio, $\nu_f W_f/\nu_o W_o$

T = temperature

U = dimensionless streamwise velocity

u = streamwise velocity

V = dimensionless transverse velocity

v = transverse velocity

W_i = molecular weight of species i

X = dimensionless streamwise coordinate

x = streamwise coordinate

Y_{fw} = wall fuel mass fraction, $(Y_{ft}B-Y_{o\infty}s)/(1+B)$

Y = dimensionless transverse coordinate

Y_i = mass fraction of species i

y = transverse coordinate

Symbols

β = Shvab-Zeldovich species coupling variable, $Y_f/\nu_f W_f - Y_o/\nu_o W_o$ or energy-species coupling variable, $-h/Q - Y_o/\nu_o W_o$

η = similarity variable

θ = dimensionless temperature, T/T_∞

κ = flow factor (0, cartesian; 1, axisymmetric)

λ = conductivity

μ = dynamic viscosity

ν = kinematic viscosity or stiochiometric coefficient

ρ = density

ψ = stream function

Subscripts

c = downstream, along centerline or wall

f = fuel

fℓ = flame

o = oxidizer

sp = stagnation plane

t = transferred gas

w = fuel surface

∞ = ambient

Superscripts

* = measured from downstream edge of fuel surface

ACKNOWLEDGEMENTS

This work was supported by the Center for Fire Research in the U.S.D.O.C. National Bureau of Standards under Grant No. NB 80 NAG-E6839 which was administered by the U.S. Department of Energy under Contract No. W-7405-ENG-48.

REFERENCES

1. Seshadri, K., and Williams, F.A.: J. Polymer Science: Polymer Chemicstry Ed., 16, 1755-1778 (1978).

2. Tsuji, H., and Yamaoka, I.: Twelfth Symposium (Int'l) on Combustion, 997-1005, The Combustion Institute (1969).

3. Tsuji, H., and Yamaoka, I.: Thirteenth Symposium (Int'l) on Combustion, 723-731, The Combustion Institute (1971).

4. Pitz, W.J., Brown, N.J., and Sawyer, R.F.: "The Structure of a Poly(ethylene) Opposed Flow Diffusion Flame" This Symposium.

5. Holve, D.J., and Sawyer, R.F.: Fifteenth Symposium (Int'l) on Combustion, 351-361, The Combustion Institute (1975).

6. Matthews, R.D., and Sawyer, R.F.: J. Fire and Flamm., 7, 200-216 (1976).

7. Milne-Thompson, L.M.: Theoretical Hydrodynamics, 5th ed., MacMillan Press, London (1968).

8. Proudman, I.: J. Fluid Mechanics, 9, 593-602 (1960).

9. Seshadri, K., and Williams, F.A.: Int. J. Heat Mass Transfer, 21, 251-253 (1978).

10. Pagni, P.J., and Shih, T.M.: Sixteenth Symposium (Int'l) on Combustion, 1329-1342, The Combustion Institute, 1976.

11. Shih, T.M., and Pagni, P.J.: ASME J. Heat Transfer, 100, 253-259 (1978).

12. Kinoshita, C.M., and Pagni, P.J.: ASME J. Heat Transfer 102, 104-109 (1980).

13. Krishnamurthy, L., and Williams, F.A.: Acta Astronautica, 1, 711-736 (1974).

14. Shih, T.M.: Numerical Heat Transfer, 2, 177-191 (1979).

15. Patankar, S.V., and Spalding, D.B.: Heat and Mass Transfer in Boundary Layers, Morgan-Grampian, West Wickham (1967).

16. Spalding, D.B.: "A General Computer Program for Two-Dimensional Boundary Layer Problems," Report No. HTS/73/48, Department of Mechanical Engineering, Imperial College of Science and Technology (1973).

17. Kinoshita, C.M.: "Development of Laminar Diffusion Flames in the Pyrolysis and Extended Flame Regions," Ph.D. Thesis, Mech. Engr. Dept., University of California, Berkeley (1979).

18. Tewarson, A., and Pion, R.F.: "A Laboratory-Scale Test Method for the Measurement of Flammability Parameters," Technical Report No. 22524, FMRC, Norwood, Mass., October 1977.

19. Tewarson, A.: "Experimental Evaluation of Flammability Parameters of Polymetric Materials," Technical Report No. 22524, RC79-T9, FMRC, Norwood, Mass., February 1979.

20. Schlichting, H.: Boundary-Layer Theory, 6th Ed., pp. 193-194, McGraw-Hill (1968).

21. Kinoshita, C.M. and Pagni, P.J., "Stagnation-Point Combustion with Radiation," This Symposium.

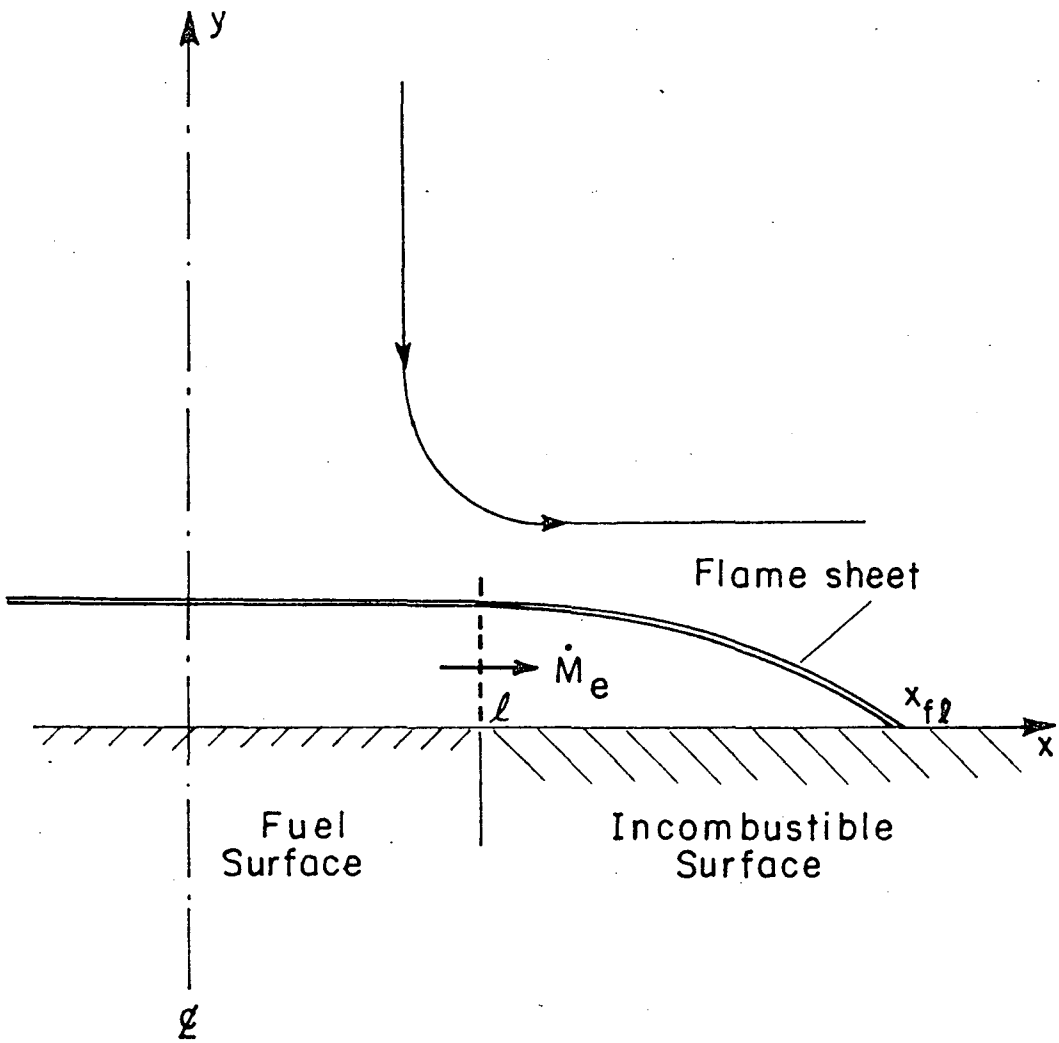

Fig. 1 System schematic of steady, laminar, opposed flow diffusion flame.

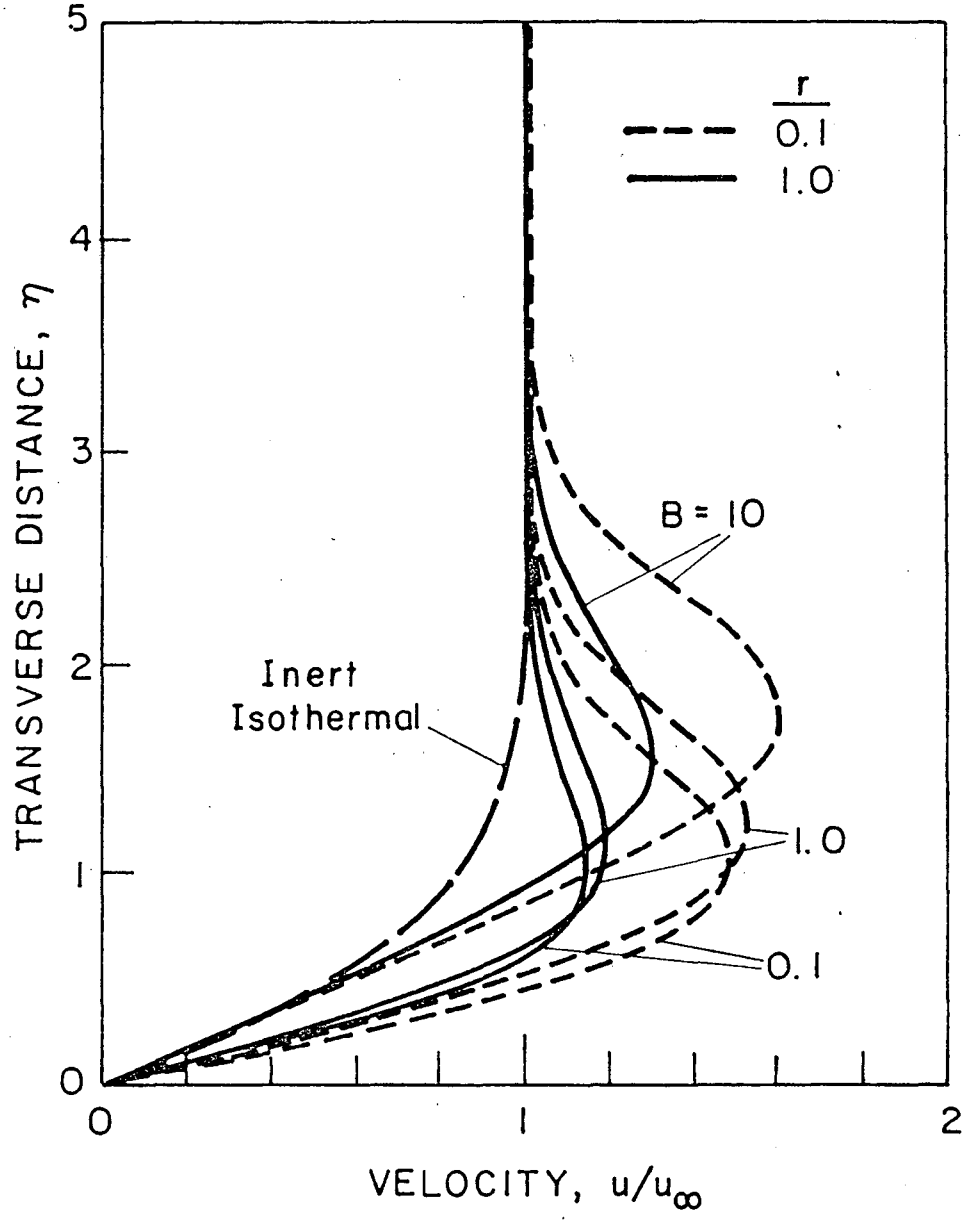

Fig. 2 Axisymmetric opposed flow diffusion flames parameterized in mass transfer and mass consumption numbers with Pr = 0.73, D_c = 4.0 and θ_w = 2.0: (a) velocity profiles; (b) temperature profiles.

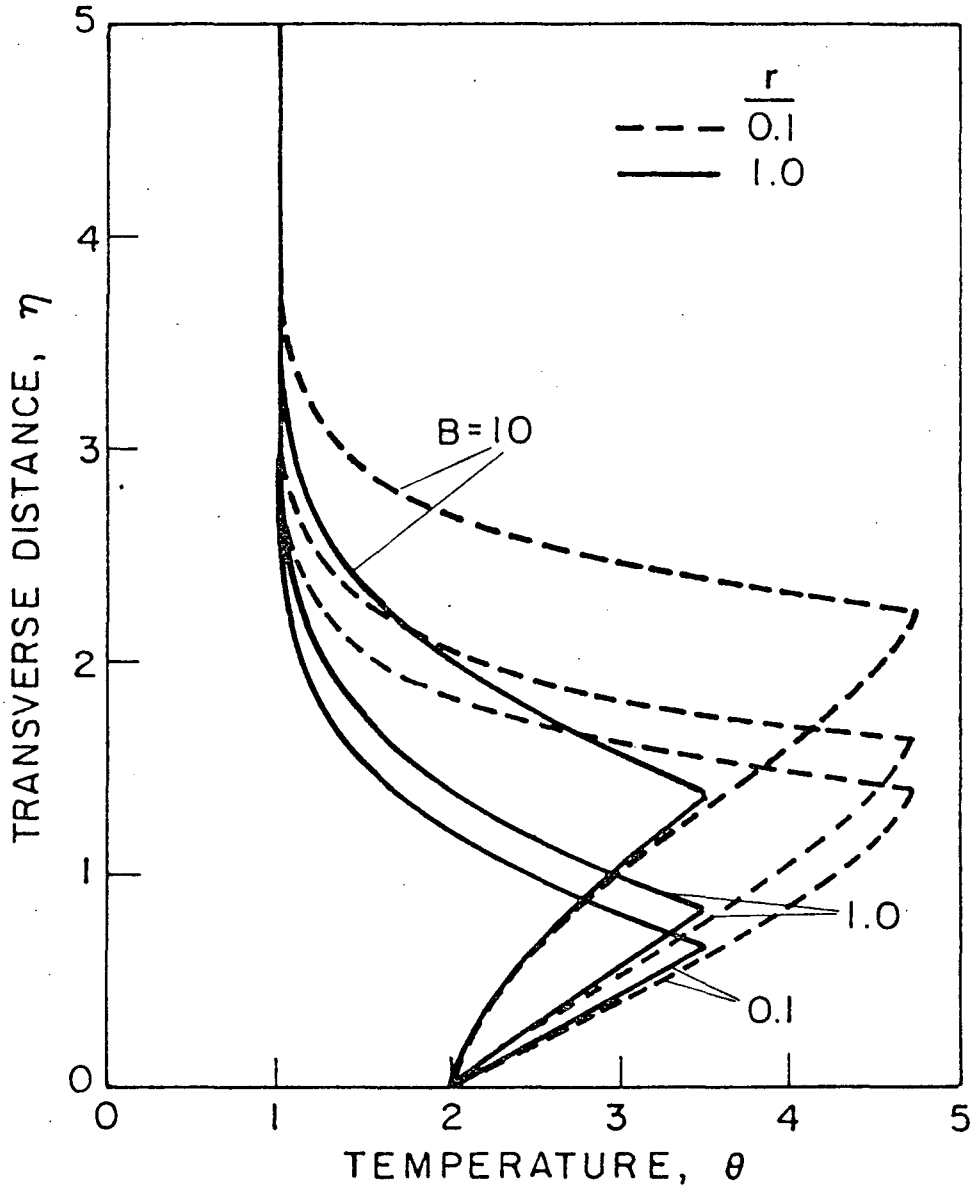

Fig. 2b

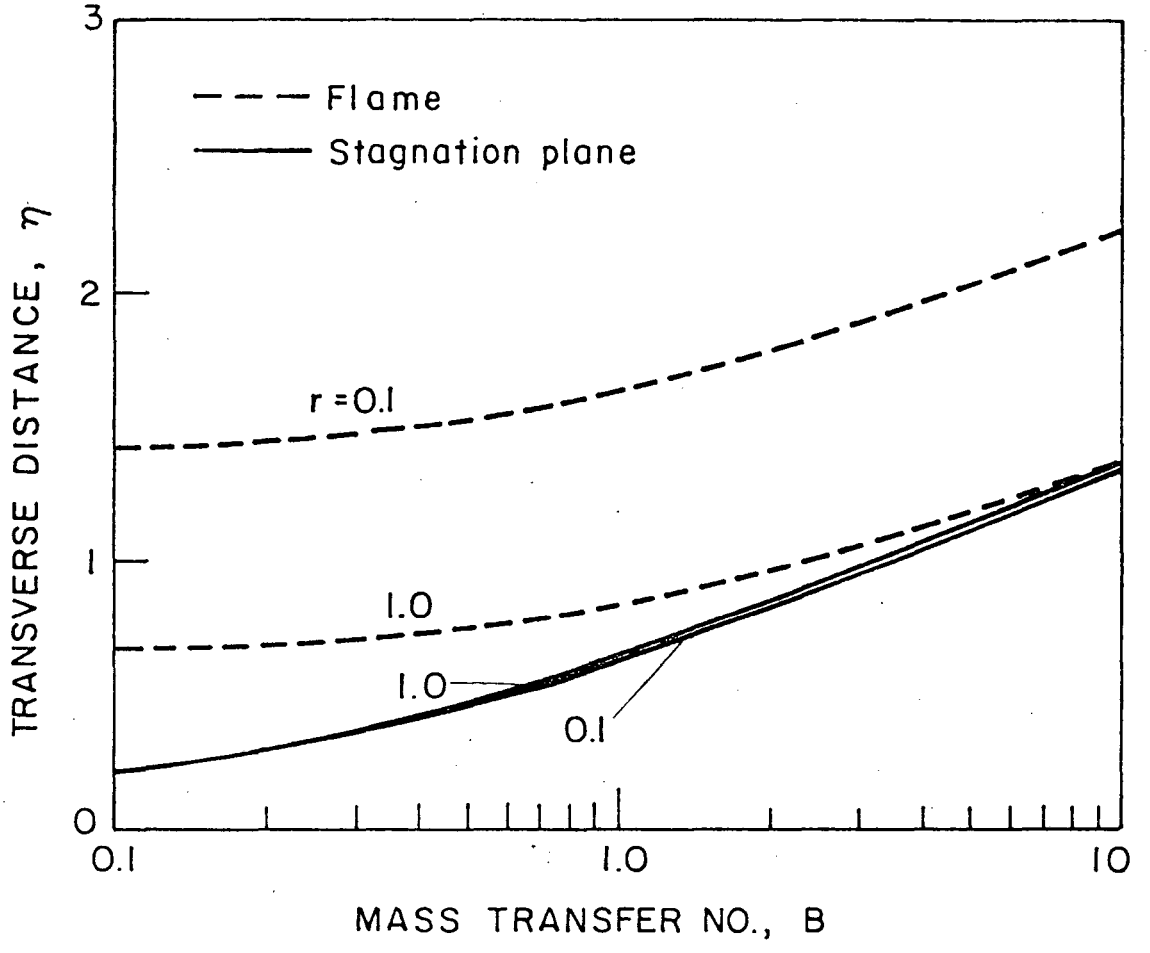

Fig. 3 Stagnation plane and flame location versus mass transfer number parameterized in mass consumption number for axisymmetric flows with Pr = 0.73, D_c = 4.0 and θ_w = 2.0.

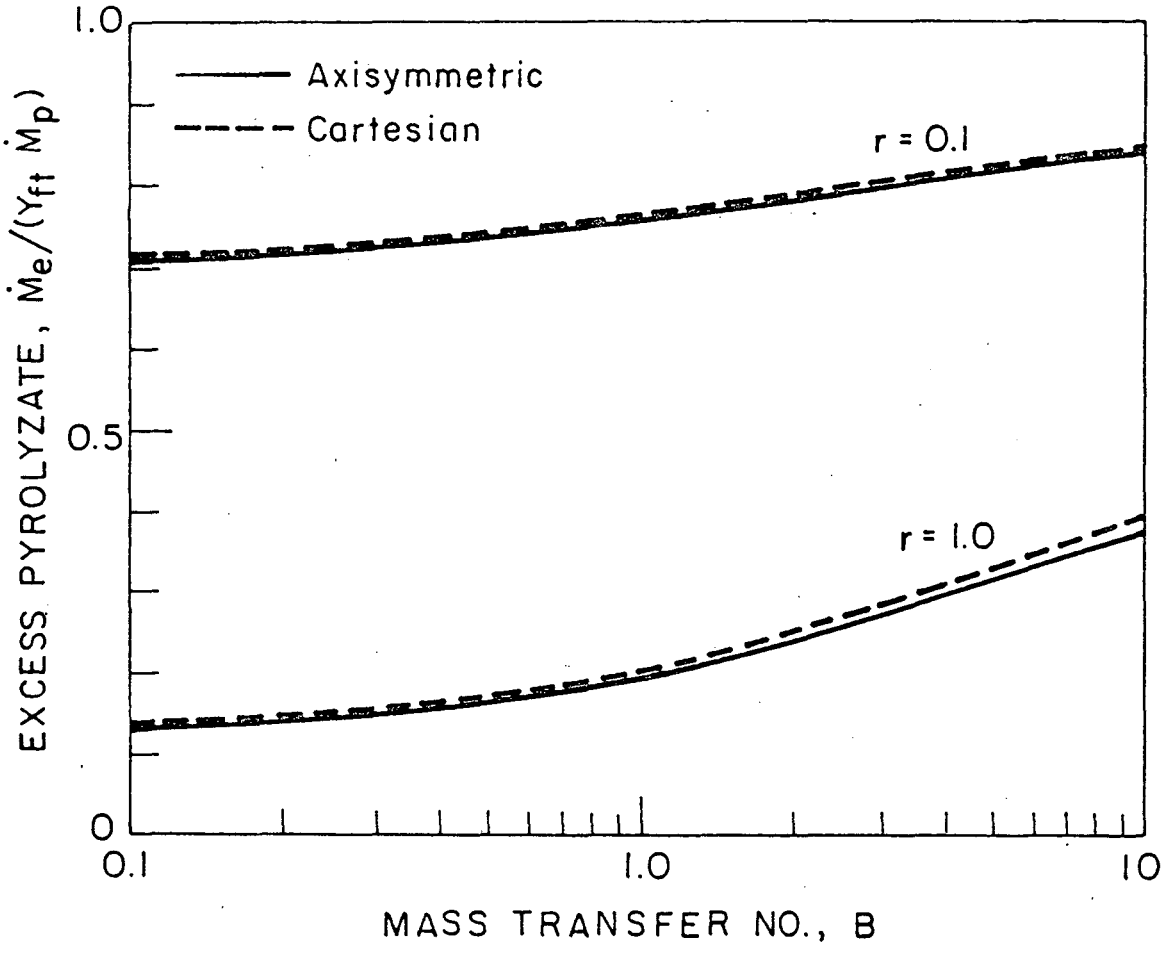

Fig. 4 Unburned pyrolyzate in pyrolysis region as fraction of total pyrolyzate versus mass transfer number parameterized in mass consumption number with Pr = 0.73, D_c = 4.0 and θ_w = 2.0.

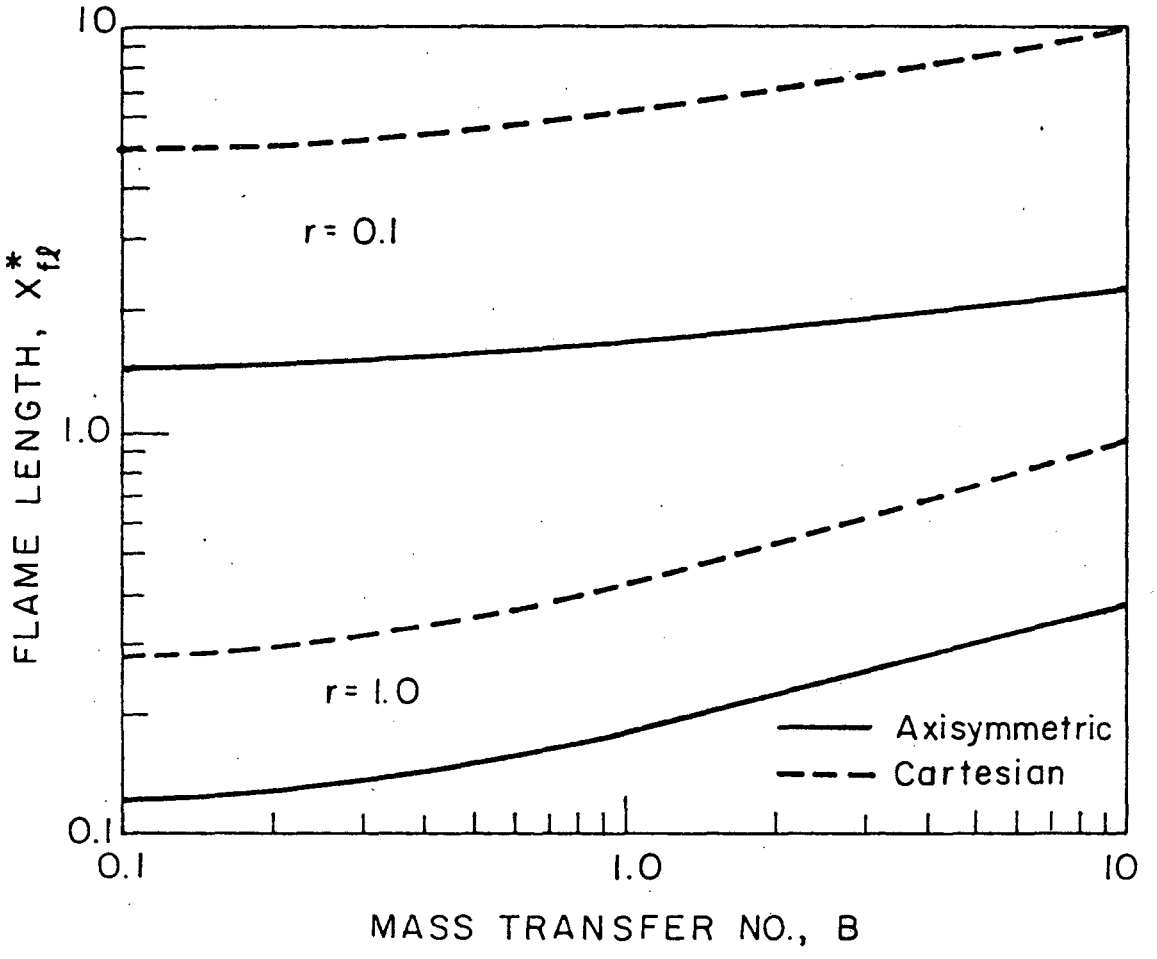

Fig. 5 Dimensionless flame extension measured from downstream edge of fuel surface versus mass transfer number parameterized in mass consumption number with Pr = 0.73, D_c = 4.0 and θ_w = 2.0.

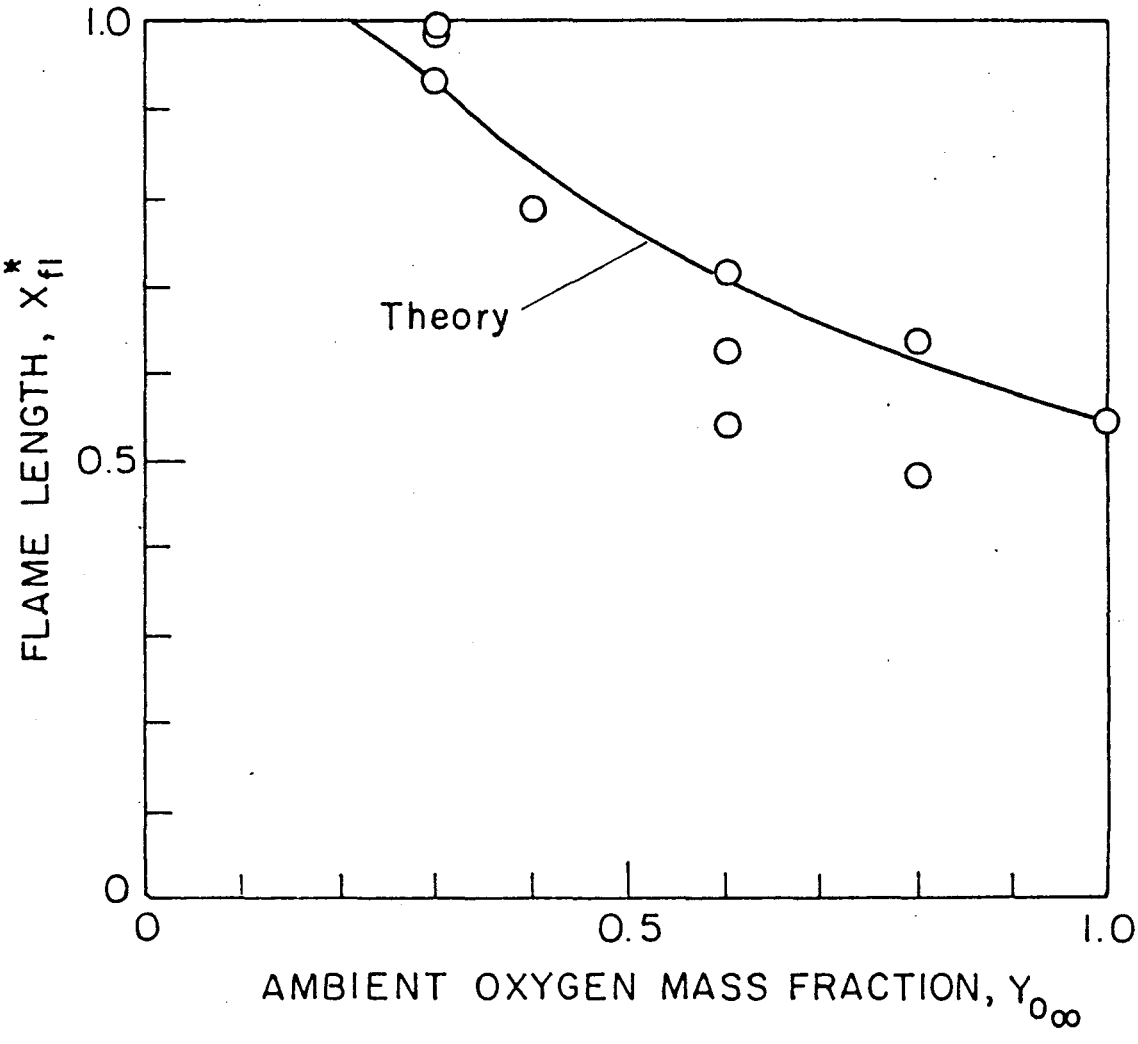

Fig. 6 Comparison of experimental and theoretical flame lengths as function of ambient oxygen mass fraction for axisymmetric PMMA OFDF's.

TECHNICAL INFORMATION DEPARTMENT
LAWRENCE BERKELEY LABORATORY
UNIVERSITY OF CALIFORNIA
BERKELEY, CALIFORNIA 94720